Evaluating and Strengthening Simple Span Girder Bridge for Heavy Lift Transportation: A Case Study of a Single Span Bridge with T-Section Reinforced Concrete

Dac Duc Nguyen
University of Transport and Communications, Hanoi, Vietnam
ngdacduc@utc.edu.vn (corresponding author)

Received: 18 February 2025 | Revised: 28 March 2025 | Accepted: 2 April 2025

 DOI: https://doi.org/10.48084/etasr.10628

ABSTRACT

The bridge construction industry has made significant progress in recent years, gradually overcoming obstacles with increasingly longer spans and higher operating loads to meet societal needs. The calculations are based on the technical specifications outlined in the design documents, the actual operating load provided by the bridge management agency, the general operating load of the entire route, and a visual assessment of the project, without considering the actual working conditions. This study explores solutions for conducting surveys, load tests, and evaluating projects to determine the response of transport loads, and applies them to simple span structures of reinforced concrete.

Keywords-evaluation; strengthening; load test; stress; strain

I. INTRODUCTION

Bridgeσ play a crucial role in the transportation network, directly impacting the socio-economic development of each country. According to statistics from the International Association for Bridge and Structural Engineering, more than 40% of the world's bridges were built more than 50 years ago and are currently facing serious deterioration [1], especially in developing countries, where budgets for bridge maintenance are limited. In addition, the increase in super-heavy transport vehicles in industry and construction poses a big challenge to the usability of old bridges. The load speed of super-heavy vehicles has been increased by an average of 20%-30% over the past two decades, exceeding the original design capacity of many bridges [13]. As a result, structural and transportation safety will continue to decline without appropriate reinforcement measures.

Simple-span reinforced concrete bridges are among the most common types of bridges, particularly in domestic road systems and older highways. The main structure of this type of bridge includes girders made of reinforced concrete, bridge bearings, a bridge deck, and a pier foundation system. With the initial design primarily intended to serve vehicles with moderate loads, many old bridges today no longer meet the requirements for transporting heavy goods due to factors, such as deterioration of material quality, designs with low safety factors, outdated load capacities, materials used, and structural forms, as well as fatigue phenomena in materials. Many bridges have been deteriorated due to the combined effects of time, environmental factors, and operational loads. According to [2], concrete strength can decrease by up to 30% after 50 years of use, while corroded reinforcement can reduce the bearing capacity of beams by up to 40%. Old bridges are often designed based on previous standards, with a lower safety factor than modern standards, and often do not consider the load of today's super-heavy vehicles. This leads to frequent overloading of bridges, increasing the risk of cracking and collapsing. Simple span bridges tend to form cracks due to fatigue effects earlier than other bridges, especially at the girder support locations and joints, as shown in Figure 1. The current condition of the T-section reinforced concrete girder bridge, designed for load H13-X60 according to 22TCN 18-79 [3], has degraded and shows signs of damage. Many strengthening methods have been investigated and applied, such as adding horizontal beams to enhance the load distribution ability and the ability to withstand horizontal collisions on the span structure [4]. Reinforcement with Fiber Reinforced Polymer (FRP) materials demonstrates that gluing Carbon Fiber Reinforced Polymer (CFRP) or Glass Fiber Reinforced Polymer (GFRP) panels to the beam surface can increase the bending capacity by 20–50%, improving structural performance without significantly increasing the bridge's weight [5].

Reinforcement with external prestressed cables helps reduce reinforcement stress and increase the load-bearing capacity of the span structure. This method is widely applied to simple girder bridge span structures and prestressed reinforced concrete [6, 7]. According to [8], applying external prestressed cables can improve the load-bearing capacity of reinforced

concrete beams by up to 40%. Strengthening by adding steel beams and installing additional steel beams parallel to the reinforced concrete beams helps redistribute loads and reduce stress on the existing structure. Many countries apply this solution due to its effectiveness and quick construction ability. Replacing bridge bearings, overlays, and deck slabs and replacing old bridge bearings with elastic or earthquake-resistant bearings enable decreasing vibrations and dynamic loads acting on beams. At the same time, replacing the bridge deck coating and old bridge deck with concrete Ultra-High-Performance Concrete (UHPC) helps reduce self-weight and improve load distribution [9].

(a)

(b)

Fig. 1. Typical damage to simple span reinforced concrete bridges: (a) damaged bridge deck, (b) damaged bridge underside.

The investigation of reinforced polymer materials was initiated in the USA in the 1930s, with the latter being widely applied to repair and strengthen reinforced concrete structures in Europe in the late 1970s. First, reinforced polymer materials replaced externally glued steel plates in steel plate gluing technology to strengthen reinforced concrete beam structures to withstand bending. Since the 1980s in Japan, this technology has been expanded to strengthen reinforced concrete columns under compression by enhancing the column's ability to restrain side expansion. Currently, reinforced polymer materials are being used for reinforced concrete slabs, with their application to steel and steel-reinforced concrete composite structures being investigated. In the past ten years, soft CFRP and GFRP materials have been widely applied for the strengthening of normal reinforced concrete and prestressed reinforced concrete girder bridge structures. Many studies have exhibited the advantages of using FRP, such as its high strengthening efficiency, quick construction, minimal machinery requirements, reduced labor demand, etc. Therefore, it is appropriate to utilize FRP materials to strengthen reinforced concrete beams, and thus meet the requirements of often transporting heavy goods.

The current study focuses on exploring a method for evaluating the load-bearing capacity of old bridges using survey data and non-destructive material testing, combined with static and dynamic load testing. Based on this evaluation, a design is proposed to increase the bearing capacity of beams to meet the demands of transporting super-heavy loads.

II. ASSESSMENT OF EXISTING BRIDGES

A. Survey, Measure Parameters, and Condition of Existing Bridges

To evaluate the load-bearing capacity of existing bridges and identify necessary reinforcement measures, the following methodology is adopted.

- Field Survey of Deck Slab and Road Surface: Cover 60 m (30 m each side) at bridgeheads using rulers (5 m, 30 m, 50 m), a generator, a drill, a thermometer, crack gauges, chalk, and a rope ladder to measure coating thickness, concrete depth, and mark damage.
- Expansion Joint Inspection: Employ similar tools plus traffic safety equipment to evaluate joint flatness and displacement capacity, identifying potential impact forces on the structure.
- Wheel Guard and Drainage Examination: Check railing, concrete edge, handrail connections, trash covers, and collection pipes for defects and damage.
- Abutment, Pier, and Foundation Evaluation: Measure cracks and defects in cap beams and piers; assess embankment settlement, transitional slab stability, slope and erosion conditions; measure tilt and displacement.
- Static Span Main Girder Inspection: Use rulers, crack gauges, and an ultrasonic crack-depth measuring device to detect and sketch cracks; check protective concrete cover, spalling, and reinforcement corrosion.
- Bridge Bearing Assessment: Inspect bearings with rulers and a panel gauge via scaffolding or ladders; evaluate rust, drainage, and displacement freedom to prevent adverse stresses.
- External Factor Survey: Record impacts of overloaded vehicles and in-bridge constructions; reference cross-sectional parameters (Figure 2) to synthesize data for structural condition assessment.
- Non-Destructive Concrete Testing: Conduct Schmidt rebound hammer tests for compressive strength, ultrasonic pulse velocity tests for homogeneity, and rebar detection for cover thickness and bar diameter on girders, abutments, and piers.

- Data Analysis and Reliability Factor (RF) Calculation: Compile survey and test results to derive structural condition factors and calculate RF values for beams, piers, and abutments.

The survey results are synthesized, analyzed, and evaluated to determine the structural condition factor used to calculate the RF value.

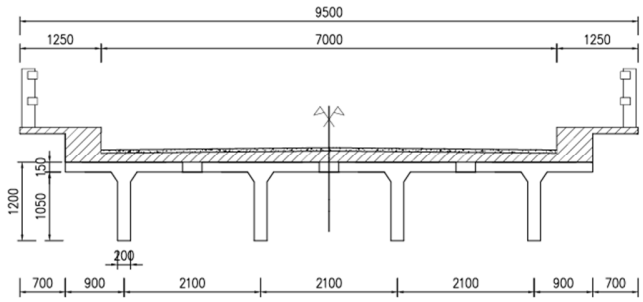

Fig. 2. A typical cross-section of span.

B. Testing the Concrete Quality of Bridge Structural Components by Non-Destructive Methods

- Non-Destructive Testing of Main Girder Concrete: Use a Schmidt rebound hammer to determine compressive strength, perform Ultrasonic Pulse Velocity (UPV) tests to assess concrete homogeneity, and employ a rebar detector to measure protective cover thickness and reinforcement diameter on representative main girders.
- Non-Destructive Testing of Abutment and Pier Concrete: Use a rebound hammer to determine compressive strength, conduct UPV tests for homogeneity, and utilize a rebar detector to measure cover thickness and bar diameter on bridge abutments and piers.

The results of testing concrete strength, protective concrete thickness, and steel diameter are compiled and utilized to calculate the RF value of the main girders and evaluate the capacity of piers and bridge abutments.

C. Determining Test Load

The test load P_{Test} (number of vehicles, vehicle load) in normal cases, should be chosen so that it satisfies the following conditions [10]:

$$0.7(1+\mu)P_{Design\ load} \le P_{Test} \le 1.2(1+\mu)\,P_{Design\ load}$$
$$\text{or } 70\% < \frac{P_{test}*100\%}{(1+\mu)} < 120\% \quad (1)$$

where P_{Test} is the moment caused by the test load and $P_{Design\ load}$ is the moment caused by the expected operating load. A four axle truck is used for testing, as illustrated in Figure 3.

A survey of the transport route shows that the bridges are all simple spans with span lengths of 15 m, 18 m, 20 m, 21 m, and 26 m, respectively. The moment value at the mid-span cross-section of the bridges should be calculated due to the transport load and the test load to evaluate the conformity. The results are portrayed in TABLE I. The calculation results show that the moment value caused by the test load is consistent with (1), so the test load used meets the requirements.

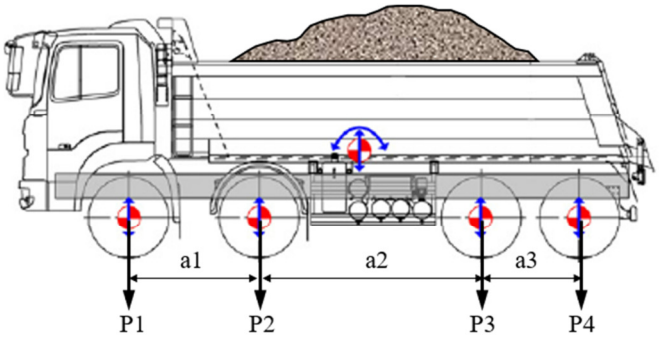

Fig. 3. Truck for bridge load test.

TABLE I. RESULTS WHEN THE LOAD TEST VEHICLE IS LOCATED AT THE BRIDGE'S CENTER AT MID-SPAN.

L (m)	**15**	**18**	**20**	**21**	**26**
IF	1.225	1.202	1.187	1.18	1.142
Truck			**Moment of beam at L/2 (kN.m)**		
DT	1839.50	2645.30	3272.10	3589.50	5176.70
HUB	1757.30	2282.00	2624.20	2795.30	3733.40
NC	1559.90	2025.70	2329.40	2481.30	3333.50
TS 1	1828.50	2629.40	3211.10	3567.90	5388.30
TS 2	1843.20	2650.70	3278.70	3596.70	5338.12
TS 3	1846.90	2656.00	3285.20	3603.90	5197.50
TS 4	1610.50	2316.00	2864.70	3142.60	4532.20
TS 5	1718.10	2255.20	2613.30	2789.40	3688.20
TF	1833.50	2601.20	3212.50	3591.10	5431.80
M_{max}	1846.90	2656.00	3285.20	3603.90	5431.80
TT	2106.00	2722.00	3131.00	3342.00	4360.00
P	93%	85%	80%	79%	70%
V	OK	OK	OK	OK	OK

TT- Test Truck , P- Percentage , V-Verification

D. Test on The Bridge

1) Dynamic Load Test

Using a device without a fixed point, vibrations are recorded in three directions: the first head measures the vibrations in the vertical direction, the second measures the vibrations in the horizontal direction across the bridge, and the third the vibrations taking place horizontally along the bridge. The measurement data are transferred to MATLAB software to plot graphs. From the graph, as shown in Figure 4, the following calculations are obtained:

- Frequency (Hz): $f = \frac{n}{t}$ (2)
- Period (s): $T = \frac{1}{f}$ (3)
- $y = \frac{y_{max}+y_{min}}{2}$ (4)
- Actual measured impact coefficient: $1+\mu = \frac{y_{max}}{y}$ (5)
- Amplitude of fluctuation: $a = \frac{y_{max}-y_{min}}{2}$ (6)

The measuring head is positioned at the top of the abutments and piers when recording their vibrations, and at the mid-span for span vibration measurements. During the load test, the vehicle moves across the bridge at a speed between 30 km/h and 40 km/h. Vibration data recording is concluded only after the response graph stabilizes and fully subsides. A

photo of the on-site vibration measurement and vibration graph is provided in Figure 5. The summary of the measured span vibration is given in Table II.

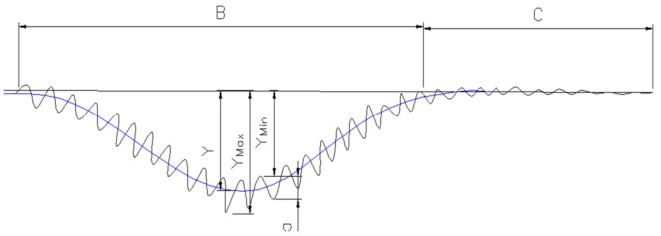

Fig. 4. Vibration measurement to calculate T, f, and a.

(a)

(b)

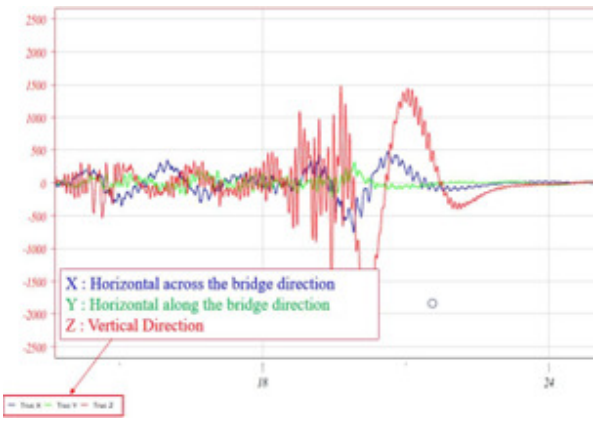

Fig. 5. (a) Typical setup for measuring vibration on site, (b) vibration graph generated by MATLAB.

According to the bridge and culvert design procedure [3], the vertical free vibration period of the spans falls outside the specified range of 0.30 s to 0.70 s; likewise, it does not comply with the 0.45 s to 0.60 s range set by the highway bridge inspection procedure [10]. The horizontal free vibration period of each span neither matches nor is an integer multiple of its vertical period, ensuring that resonance cannot occur when vehicles pass over the bridge. Moreover, the dynamic coefficient measured at mid-span (1 + IM) is below the 1.33 limit, as specified in [11].

TABLE II. STRUCTURAL VIBRATION MEASUREMENT RESULTS OF THE BRIDGE SPAN

Span	Direction	T (s)	Z_{max}	Z_{min}	1+μ
N1	Vertical	0.1598	3.975	2.306	1.2657
	Horizontal across the bridge	0.1857			
	Horizontal along the bridge	0.2061			
N2	Vertical	0.1594	3.289	1.903	1.2669
	Horizontal across the bridge	0.1852			
	Horizontal along the bridge	0.2068			

2) Static Test

The stress is measured using a clock that combines a 200 mm standard gauge with 1000-fold amplification, while the deflection of the main girder is measured using a clock with 100-fold amplification, as displayed in Figure 6. The analysis and evaluation results are compared with the limit values according to the procedure, and the conclusion is the load-bearing capacity of the bridge under the effect of the test load.

Fig. 6. Photo of deflection and strain measurement gauge.

The stress is calculated based on the measured strain, considering the elastic modulus of the concrete (MPa) girder according to [11]:

$$Eb = 0.0017\gamma_c^2\sqrt{f_c'} = 31{,}260 \quad (7)$$

where γc is the specific volume of concrete (2400 kg/m^3) and f_c' is the compressive strength of concrete (33.7 MPa).

Based on the deflection measurement results, the actual horizontal distribution coefficient for the girders at the mid-span section is calculated, as shown in Figure 7. The actual measured horizontal distribution coefficient is calculated by:

$$\eta_k = \frac{f_k}{\sum f_i} \quad (8)$$

where η_k measures the horizontal distribution coefficient of girder k, fk denotes the girder deflection k, $\sum f_i$ is the total deflection of the girders on the cross-section. The results of measuring the horizontal distribution coefficient, as portrayed in Figure 7, indicate that although the test load is placed near the center-right of the span, it is unevenly distributed across the

beams due to the absence of cross beams in the bridge structure. The bridge deck concrete is degraded, leading to failure to meet the load distribution requirements.

E. The Results of The Calculation of the Rating Factor

The Rating Factor (RF) is calculated according to the survey results of the structural and material parameters along with the actual measured horizontal distribution coefficient. The results are summarized in Table III. According to [12], the general principle for bridge structures is that the assessment calculation is carried out based on the bridge limit state for all vehicles and transport loads. The general formula is:

$$RF = \frac{C-DL}{LL} = \frac{HL}{LL} \quad (9)$$

where RF is the rating factor, C is the load bearing capacity of the rated member, DL is the permanent load effect, and LL is the live load effect. HL is the load-bearing capacity and is given by:

$$HL = C - DL \quad (10)$$

The calculation sequence is shown in the diagram demonstrated in Figure 8.

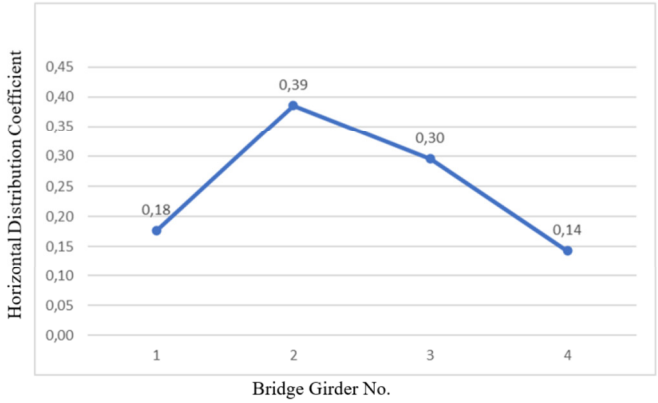

Fig. 7. Bridge horizontal distribution.

The calculation results, presented in Table III, show that the RF value is less than 1 in some transport loads, such as the Drive train, TS1, TS2, TS3, and Transformer. The RF is the smallest when transporting the Transformer, so it is necessary to strengthen the design to reach an RF greater than 1.

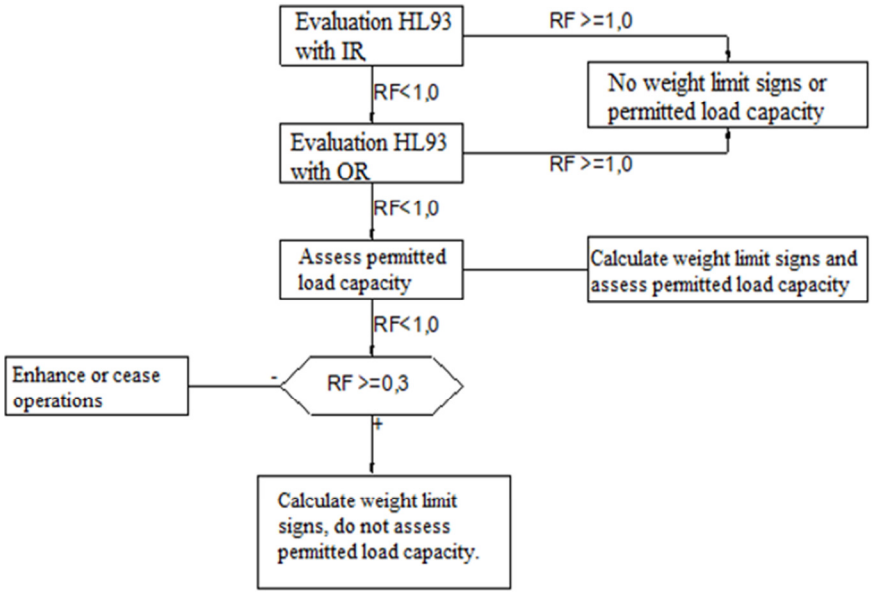

Fig. 8. Calculation sequence to determine RF.

TABLE III. RESULTS OF THE FLEXURAL CAPACITY

Load case	CM (kN·m)	M_{DL} (kNm)			M_{LL} (kNm)			RF
	$FcFsM_N$	g_{DC}	M_{DC}	g_{DW}	M_{DW}	g_{LL}	M_{LL+IM}	
HL-93-IR	1914.84	1.25	361.74	1.50	323.26	1.75	114.43	0.55
HL-93-OR	1914.84	1.25	361.74	1.50	323.26	1.35	114.43	0.71
Drive Train	1914.84	1.25	361.74	1.50	323.26	1.10	911.10	0.98
HUB	1914.84	1.25	361.74	1.50	323.26	1.10	870.39	1.02
NACELLE	1914.84	1.25	361.74	1.50	323.26	1.10	772.62	1.15
TS 1	1914.84	1.25	361.74	1.50	323.26	1.10	905.66	0.98
TS 2	1914.84	1.25	361.74	1.50	323.26	1.10	912.94	0.97
TS 3	1914.84	1.25	361.74	1.50	323.26	1.10	914.77	0.97
TS 4	1914.84	1.25	361.74	1.50	323.26	1.10	797.68	1.11
TS 5	1914.84	1.25	361.74	1.50	323.26	1.10	850.97	1.04
TS 6	1914.84	1.25	361.74	1.50	323.26	1.10	850.97	1.04
Transformer	1914.84	1.25	361.74	1.50	323.26	1.10	1095.80	0.81

TABLE IV. RESULTS OF RF CALCULATION AFTER STRENGTHENING APPLICATION

Load case	CM (kN·m)	M_{DL} (kNm)			M_{LL} (kNm)			RF
	$FcFsM_N$	g_{DC}	M_{DC}	g_{DW}	M_{DW}	g_{LL}	M_{LL+IM}	
HL-93-IR	2174.33	1.25	361.74	1.50	323.26	1.75	114.43	0.70
HL-93-OR	2174.33	1.25	361.74	1.50	323.26	1.35	114.43	0.90
Drive Train	2174.33	1.25	361.74	1.50	323.26	1.10	911.10	0.98
HUB	2174.33	1.25	361.74	1.50	323.26	1.10	870.39	1.23
NACELLE	2174.33	1.25	361.74	1.50	323.26	1.10	772.62	1.29
TS 1	2174.33	1.25	361.74	1.50	323.26	1.10	905.66	1.46
TS 2	2174.33	1.25	361.74	1.50	323.26	1.10	912.94	1.24
TS 3	2174.33	1.25	361.74	1.50	323.26	1.10	914.77	1.23
TS 4	2174.33	1.25	361.74	1.50	323.26	1.10	797.68	1.41
TS 5	2174.33	1.25	361.74	1.50	323.26	1.10	850.97	1.32
TS 6	2174.33	1.25	361.74	1.50	323.26	1.10	850.97	1.32
Transformer	2174.33	1.25	361.74	1.50	323.26	1.10	1095.80	1.00

III. STRENGTHENING THE MAIN GIRDERS

A. Design Strengthening

Based on the load test results and the urgent need for strengthening to meet the transportation demands, the selected solution involves adding a 10 mm thick steel plate on the bridge deck to improve load distribution, along with applying three layers of FRP fibers at the bottom of the beam to enhance its moment-bearing capacity, as illustrated in Figure 9. The ultimate tensile strength in the primary fiber direction of design value is 834 MPa.

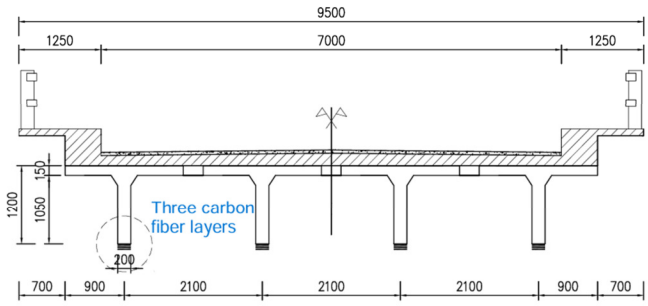

Fig. 9. The cross-section after strengthening with three carbon fiber layers.

Fig. 10. Beam after application of carbon fiber reinforcement.

The carbon fiber layer construction process includes cleaning the surface bottom of the girder and applying Sika Latex to patch pits. After filling the chipped edges and rough bottoms of beams with TKA-Monos high-strength mortar, the bottom of the beam is ground to become flat, dust is blown to clean the bottom of the beam, while Tyfo S glue is applied onto the beam and fiber surfaces. Following this, the fiber is glued to the bottom surface of the girder. Fiber maintenance rolling ensures that the fibers stick evenly on the beam surface. The results obtained after the RF addition are shown in Figure 10.

B. Post-Assessment After Strengthening

After the carbon fiber strengthening, a load test is conducted to measure stress and deflection. Based on these measurements, the actual horizontal distribution coefficient is determined, and the RF are calculated. The results are presented in Figure 11.

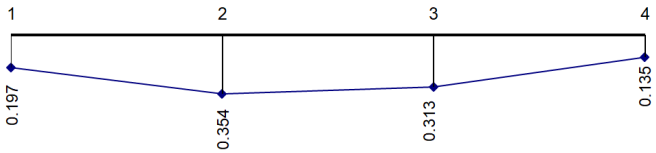

Fig. 11. Horizontal load distribution of the bridge after strengthening.

After strengthening, the horizontal distribution coefficient diagram shows that the load distribution value for Girder No. 2 decreases from 0.39 to 0.354, representing a reduction of 9.23%. Table IV illustrates the results of the re-evaluation of the RF using the actual measured horizontal distribution coefficient after reinforcing the girder with three layers of FRP fibers.

The calculation results of the RF value after adding steel plates to the bridge deck and strengthening three layers of carbon fiber are demonstrated in TABLE IV. The results indicate that the minimum RF is 1.0 when transporting the transformer, demonstrating that the project meets the transportation requirements.

IV. CONCLUSION

For overweight goods, besides minimizing cargo weight and designing transport vehicles to distribute the load along the longitudinal direction of the bridge, it is also necessary to

research and evaluate possible solutions to strengthen the bridges in accordance with the transportation plan, in order to achieve an optimal solution. The assessment of strengthening an old bridge must be carefully carried out according to the following steps: conduct a detailed survey of the size and current condition of the bridge; perform tests to evaluate the quality of the concrete and reinforcement; and measure the horizontal distribution coefficient to calculate the RF based on the actual measured results. If the RF is less than 1, propose appropriate strengthening solutions, then re-test and re-evaluate the RF. If the RF is greater than 1, the span structure is considered sufficient to meet the transport load requirements.

Applying the results of the evaluation study to the T-section reinforced concrete girder bridges constructed since the 1980s shows that based on the initial evaluation with HL-93-IR, and HL-93-OR loads, all RF coefficients are less than 1.0. Conducting evaluation by using 10 types of transport loads based on bridge structural condition reveals that the smallest RF value is 0.81. This indicates that adding steel plates to distribute the bridge deck load, as well as increasing the carbon fiber at the bottom of the girders, is necessary to achieve an RF value of 1.0, thereby meeting the transport requirements.

CONFLICT OF INTEREST

The authors declare that they have no conflicts of interest regarding the publication of this paper.

REFERENCES

[1] H. H. (Bert) Snijder and B. De Pauw, "IABSE Congress Ghent 2021 'Structural Engineering for Future Societal Needs," Structural Engineering International, vol. 32, no. 1, Jan. 2022, Art. no. 112–115, https://doi.org/10.1080/10168664.2022.2016290.

[2] B. Lee, J.-S. Lee, and J.-S. Ryou, "Long-term Compressive Strength Properties of Concrete Incorporating Admixtures: Outdoor Exposure Testing in a Coastal Environment," International Journal of Concrete Structures and Materials, vol. 18, no. 1, 54, Aug. 2024, Art. no. 112–115, https://doi.org/10.1186/s40069-024-00687-8.

[3] "22TCN 18-79: Bridge and Culvert Structure Design Standards According to Limit States." Vietnam, 1979.

[4] N. Duc and H. Minh, "Investigation on the effect of cross beams in single span bridges under dynamic aspect by using finite element method," *Journal of Materials and Engineering Structures*, vol. 9, no. 4, 435–445, Dec. 2022, Art. no. 112–115.

[5] F. Peng, W. Xue, and T. Yu, "Cyclic behavior of polypropylene fiber reinforced concrete beams with prestressed CFRP tendons and nonprestressed steel bars," *Engineering Structures*, vol. 275, Jan. 2023, Art. no 115201, https://doi.org/10.1016/j.engstruct.2022.115201.

[6] D. D. Nguyen and V. H. Tran, "Repair and Strengthening of Cantilever Continuous Bridges using External Prestressed Cables: The Case Study of the Tan De Bridge in Vietnam," *Engineering, Technology & Applied Science Research*, vol. 15, no. 1, Feb. 2025, Art. no 20005–20011, https://doi.org/10.48084/etasr.9536.

[7] H. Hoang, V. Hoang, and D. H. Nguyen, "Long-Term Monitoring of Cable Tension Force in Cable-stayed Bridges using the Vibration Method. The Case Study of Binh Bridge, Vietnam," *Engineering, Technology & Applied Science Research*, vol. 15, no. 1, Feb. 2025, Art. no. 20300–20313, https://doi.org/10.48084/etasr.9737.

[8] S. Seręga and D. H. Faustmann, "Flexural strengthening of reinforced concrete beams using external tendons," *Engineering Structures*, vol. 252, Feb. 2022, Art. no. 113277, https://doi.org/10.1016/j.engstruct. 2021.113277.

[9] Y. Zhang and Y. H. Chai, "Numerical analysis of bridge deck rehabilitation by ultra-high-performance concrete (UHPC) overlay," *Structures*, vol. 33, Oct. 2021, Art. no. 4791–4802, https://doi.org/10.1016/j.istruc.2021.07.044.

[10] "22TCN 243-98: Procedure for inspection of bridges on motor roads – technical requirements." Vietnam, 1998.

[11] "TCVN 11823:2017 – Highway bridge design specification." Vietnam, 2017.

[12] "TCVN 12882:2020 – Standards for assessing the bearing capacity of road bridges." Vietnam, 2020.

[13] LRFD bridge design specification. Washington, DC, USA: AASHTO, 2020.